

MimCo: Masked Image Modeling Pre-training with Contrastive Teacher

Qiang Zhou
Alibaba Group
Hangzhou, China
jianchong.zq@alibaba-inc.com

Chaohui Yu
Alibaba Group
Hangzhou, China
huakun.ych@alibaba-inc.com

Hao Luo
Alibaba Group
Hangzhou, China
michuan.lh@alibaba-inc.com

Zhibin Wang[✉]
Alibaba Group
Hangzhou, China
zhibin.waz@alibaba-inc.com

Hao Li
Alibaba Group
Hangzhou, China
lihao.lh@alibaba-inc.com

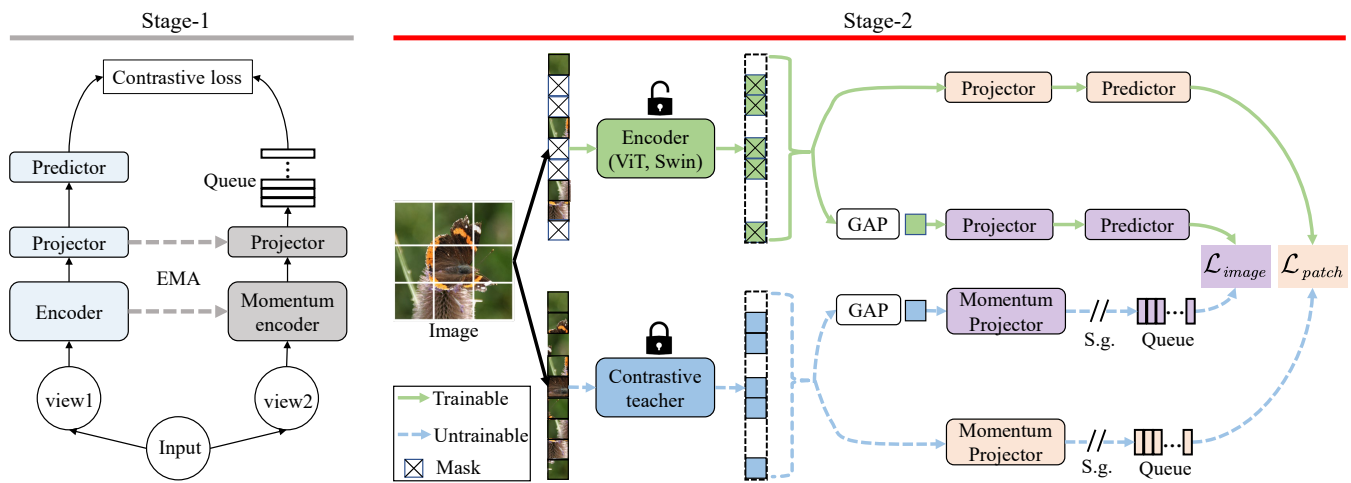


Figure 1: The proposed pre-training framework MimCo. MimCo is pre-trained in two stages. The first stage (Stage-1) denotes contrastive learning-based pre-training, e.g., MoCov3 [9], MoBY [43]. The second stage (Stage-2) is our main framework, which uses the pre-trained encoder in stage-1 as a contrastive teacher. “S.g.” denotes stop gradient, “GAP” is a global average pooling layer.

ABSTRACT

Recent masked image modeling (MIM) has received much attention in self-supervised learning (SSL), which requires the target model to recover the masked part of the input image. Although MIM-based pre-training methods achieve new state-of-the-art performance when transferred to many downstream tasks, the visualizations show that the learned representations are less separable, especially compared to those based on contrastive learning pre-training. This

inspires us to think whether the linear separability of MIM pre-trained representation can be further improved, thereby improving the pre-training performance. Since MIM and contrastive learning tend to utilize different data augmentations and training strategies, combining these two pretext tasks is not trivial. In this work, we propose a novel and flexible pre-training framework, named MimCo, which combines MIM and contrastive learning through two-stage pre-training. Specifically, MimCo takes a pre-trained contrastive learning model as the teacher model and is pre-trained with two types of learning targets: patch-level and image-level reconstruction losses.

Extensive transfer experiments on downstream tasks demonstrate the superior performance of our MimCo pre-training framework. Taking ViT-S as an example, when using the pre-trained MoCov3-ViT-S as the teacher model, MimCo only needs 100 epochs of pre-training to achieve 82.53% top-1 finetuning accuracy on Imagenet-1K, which outperforms the state-of-the-art self-supervised learning counterparts.

[✉] Corresponding author.

Permission to make digital or hard copies of all or part of this work for personal or classroom use is granted without fee provided that copies are not made or distributed for profit or commercial advantage and that copies bear this notice and the full citation on the first page. Copyrights for components of this work owned by others than ACM must be honored. Abstracting with credit is permitted. To copy otherwise, or republish, to post on servers or to redistribute to lists, requires prior specific permission and/or a fee. Request permissions from permissions@acm.org.

MM '22, October 10–14, 2022, Lisboa, Portugal

© 2022 Association for Computing Machinery.

ACM ISBN XXXXXX/XX/XX...\$15.00

<https://doi.org/XXXXXXXX.XXXXXXX>

CCS CONCEPTS

• **Computing methodologies** → **Image representations.**

KEYWORDS

self-supervised learning, pre-training, contrastive learning, mask image modeling

ACM Reference Format:

Qiang Zhou, Chaohui Yu, Hao Luo, Zhibin Wang[✉], and Hao Li. 2022. MimCo: Masked Image Modeling Pre-training with Contrastive Teacher. In *Proceedings of the 30th ACM International Conference on Multimedia (MM '22), October 10–14, 2022, Lisboa, Portugal*. ACM, New York, NY, USA, 9 pages. <https://doi.org/XXXXXXX.XXXXXXX>

1 INTRODUCTION

With the development of deep neural networks [22] and transformers [38], masked language modeling (MLM) has achieved great success and emerged as an important self-supervised pre-training approach for language models in natural language processing (NLP). For instance, BERT [11] innovatively proposes to randomly mask a part of the input sequence and learn to predict or reconstruct these masked tokens, which has almost become the standard pre-training paradigm in NLP. Inspired by the success of MLM, recently, masked image modeling (MIM) has achieved fast development in visual pre-training tasks, showing the potential to be an important training paradigm for self-supervised learning in vision.

MIM is a task of randomly masking some patches of an input image and learning to reconstruct the masked patches. ViT [14] and BEiT [3] propose to perform MIM in self-supervised pre-training with vision transformer (ViT) [14]. BEiT first proposes to use a trained discrete variational autoencoder (dVAE) [33] to build a visual vocabulary, imitating the language vocabulary in NLP, which provides promising performance in visual pre-training. Following BEiT, very recently, several MIM literature have been proposed to further promote the self-supervised learning in vision. Some methods [19, 45] propose to directly regress the raw pixels of the masked patches in a simple and effective way. Other methods [13, 40, 47] turn to improve the semantic of visual tokens.

Although state-of-the-art MIM-based self-supervised learning methods achieve impressive performance when transferred to downstream tasks, they suffer from **poor linear separability of learned representations**, as shown in Figure 3. The linear separability of representations is highly correlated with transfer performance for tasks that require frozen features, such as image retrieval. It is not surprising that recent MIM-based pre-training work [45] has limited performance on these downstream tasks. In contrast, the learned representations are more linearly separable based on the contrastive learning pre-training paradigm, *e.g.*, MoBY [43] and MoCov3 [9]. This motivates us to combine these two pre-training paradigms of MIM and contrastive learning and propose a new pre-training framework.

However, introducing contrastive learning into MIM is not trivial since MIM and contrastive learning tend to utilize different data augmentations and training strategies. In this work, we propose a novel and flexible pre-training framework, named MimCo. As show in Figure 1, MimCo is pre-trained in two stages. In the first stage, the contrastive teacher model is pre-trained based on contrastive

learning methods, such as MoCov3 [9], MoBY [43], *etc.* In the second stage, MimCo is pre-trained with MIM, and the contrastive teacher model will not be updated, which is similar to the role of dVAE [33] in BEiT [3]. Through decoupling the MIM and contrastive learning paradigms, MimCo is more flexible and efficiency during pre-training. First, MIM and contrastive learning are two different pre-training paradigms, differing vastly from data augmentations to training hyperparameters. Thus pre-training them individually is more convenient and flexible. Second, advances in contrastive learning based pre-training will benefit MimCo by simply replacing the contrastive teacher with a new and better model.

To take full advantage of the contrastive teacher model, we further propose two types of reconstruction losses. The first is the **patch-level** reconstruction loss. For the masked patches, we take the corresponding features of the contrastive teacher model as reconstruction targets. Compared to directly predicting the patch features [40], we propose to reconstruct the patch features through a contrastive loss, which performs better. The second is the **image-level** reconstruction loss, which reconstructs the overall features of the masked image. The image-level reconstruction, also implemented as a contrastive loss, helps improve the linear separability of learned representations, as shown in Table 9.

Overall, this work makes the following contributions:

- We propose a novel and flexible pre-training framework, named MimCo, which takes a contrastive learning pre-trained model as the teacher model. Compared with recent MIM pre-training methods, MimCo owns more separable representations and better transfer performances.
- To take full advantage of the contrastive teacher model, we propose two reconstruction losses, *i.e.*, patch-level and image-level, which are experimentally verified to be effective.
- Extensive experiments on many downstream tasks, including classification, object detection, instance segmentation, and semantic segmentation demonstrate that our MimCo pre-training framework can achieve superior transfer performance against state-of-the-art methods.

2 RELATED WORK

During the booming of deep learning, recent years have witnessed remarkable progress of self-supervised learning (SSL) [12, 17, 27, 29, 30, 39, 46].

Contrastive Learning Pre-training. Recently, one line of research focus on contrastive learning [1] based pre-training methods, and plenty of literature [4, 7, 15, 18, 20, 37, 41, 43, 44] have been proposed, which dominate the previous self-supervised visual representation learning. These methods learn discriminative representation by attracting similar instances and dispelling dissimilar instances, based on two or multiple different augmented views of one image. For instance, SimCLR [7] proposes a simple framework to promote the performance of self-supervised learning by maximizing the mutual information between two augmented views of a image. MoCo [20] uses a momentum encoder to maintain consistent representations of negative pairs drawn from a memory bank, which enables building a large and consistent dictionary on-the-fly that facilitates contrastive unsupervised learning. BYOL [18] proposes a metric-learning manner, which uses a moving average

network to produce prediction targets as a means of stabilizing the bootstrap step. MoBY [43] proposes an elegant combination of MoCo [20] and BYOL [18], with a proper training recipe and lighter tricks, MoBY can achieve high performance. Our method takes the contrastive learning pre-trained model as the teacher model and aims to improve the performance of MIM pre-training.

Masked Image Modeling Pre-training. Masked language modeling (MLM) methods [11, 32] often mask some part of the input sequence and then train the models to model the missing portion. MLM methods have been a popular language model pre-training paradigm in NLP. Inspired by the great success of modern MLM methods in NLP, very recently, another line of research on self-supervised visual learning tends to masked image modeling (MIM). iGPT [6] trains a sequence Transformer [38] to auto-regressively predict the next pixels and learns state-of-the-art representations for low resolution datasets. ViT [14] proposes to predict mean color of each corrupted patch using their respective patch representations with ViT. BEiT [3] proposes to use a pre-trained discrete variational autoencoder (dVAE) [33], which can be seen as a offline tokenizer, to encode masked patches. Following BEiT [3], MAE [19] develops an asymmetric encoder-decoder architecture to reconstruct the normalized masked patches. SimMIM [45] propose a simple framework to reconstruct the raw pixels. iBOT [47] performs masked image modeling via self-distillation by introducing an online tokenizer. PeCo [13] proposes to learn a perceptual codebook, which exhibits better semantic meanings of the visual tokens. MaskFeat [40] presents masked feature prediction with HOG [10] for self-supervised pre-training of video models. Our method is complementary to the MIM methods.

Self-supervised Learning and Knowledge Distillation. Knowledge distillation (KD) [2, 23] aims to distill knowledge from a well-trained model (teacher) to another model (student). Typical KD methods usually leverage the intermediate features or the output logits of a teacher model to supervise the training of a student model. Hinton et al. [23] first proposes to distill knowledge from teacher’s output logits into smaller student model. FitNets [34] extend this idea to distill the knowledge via minimizing the intermediate features learned by the teacher and the student model. Recently, some works introduce the KD methods into self-supervised learning [8, 16, 24, 28, 35]. [28] proposes a knowledge transfer method to decouple the pre-training model and the final task model based on clustering the learned features. [35] proposes to use contrastive loss to learn cross-modality consistency. CompRes [24] compresses an already learned deep self-supervised teacher model into a smaller student model by mimicking the relative similarity of data points in the teacher’s embedding space. SEED [16] first trains a large network in a self-supervised fashion, and then trains a small network to mimic the similarity score distribution inferred by the large network over a set of instances. DINO [5] proposes to simplify self-supervised training by directly predicting the output of a teacher network, which is built with a momentum encoder. In this work, we propose to extract knowledge from pre-trained contrastive teacher models when performing MIM pre-training.

3 APPROACH

We inspire our method by improving the performance of MIM pre-training with the assistance of contrastive learning. Instead of combining MIM and contrastive learning via multi-task learning, we propose a novel two-stage pre-training framework that is more flexible and achieves higher performance. In this section, we elaborate the framework, learning targets, and implementation details of MimCo, respectively.

3.1 Framework

MimCo is pre-trained in two-stages. In the first stage, we use contrastive learning methods, such as MoCov3 [9], MOBY [43], etc., to pre-train on the ImageNet-1K dataset. The pre-trained model will be used as the contrastive teacher model in our MimCo pre-training, as shown in Figure 1. We refer readers to these works for more details, and in our experiments, we directly use the open-source models from these works.

As shown in Figure 1, MimCo mainly consists of a learnable encoder f , a frozen contrastive teacher model f' , and two sets of contrastive learning modules. During pre-training, for each training sample x , we first randomly generate a mask m using the same masking strategy as in SimMIM [45]. Then, the contrastive teacher model takes as input the non-masked image and extracts features $f'(x)$, while the learnable encoder extracts features $f(x, m)$ for the masked image using the generated mask m . The non-masked features $f'(x)$ will be used as the targets to reconstruct the masked feature $f(x, m)$ through patch-level and image-level reconstruction losses, which will be described in the next section. After pre-training, only the learnable encoder is applied to non-masked images to extract representations for downstream tasks.

3.2 Learning Targets

In this section, we elaborate the learning targets of MimCo, including the patch-level and image-level reconstruction losses. Algorithm 1 provides the pseudo-code of MimCo for these learning targets.

Patch-level Reconstruction Loss. Similar to other MIM-based SSL work [19, 45], we reconstruct knowledge for those masked patches of input sample x . MaskFeat [40] verifies that reconstructing the features of the a pre-trained model via ℓ_1 -loss is better than directly reconstructing the raw pixels or HOG features. Unlike MaskFeat, we experimentally find that reconstructing the features via contrastive loss is superior to ℓ_1 -loss, as shown in Table 7. To be specific, we adopt a contrastive learning loss to model the similarity of the local patches between masked and non-masked images. Following MoBY [43], a projector p_1^p (2 layer convolution), a predictor p_2^p (2 layer convolution), and a momentum projector p_3^p (2 layer convolution) are introduced when computing the contrastive loss, as shown in Figure 1. Formally, the patch-level reconstruction loss $\mathcal{L}_{\text{patch}}$ can be computed as follows. For convenience, we show the $\mathcal{L}_{\text{patch}}$ computed on one input sample x .

$$\mathcal{L}_{\text{patch}} = \frac{1}{M} \sum_{i=1}^M -\log \frac{\exp(q_i \cdot k_{(i,+)} / \tau)}{\exp(q_i \cdot k_{(i,+)} / \tau) + \sum_{j=1}^K \exp(q_j \cdot k_j / \tau)}, \quad (1)$$

in which:

$$\begin{cases} q_i = \mathbf{p}_2^p(\mathbf{p}_1^p(\mathbf{f}(x, m)))_i, \\ k_{i,+} = \mathbf{p}_3^p(\mathbf{f}'(x))_i, \end{cases} \quad (2)$$

where M denotes the total number of masked patches of a sample x . $m \in \mathbb{R}^{1 \times \frac{H}{P} \times \frac{W}{P}}$ is the randomly generated mask applied to x . $\{\mathbf{p}_2^p(\mathbf{p}_1^p(\mathbf{f}(x, m))), \mathbf{p}_3^p(\mathbf{f}'(x))\} \in \mathbb{R}^{C \times \frac{H}{P} \times \frac{W}{P}}$ are the output features of the predictor \mathbf{p}_2^p and momentum projector \mathbf{p}_3^p , respectively. P denotes the patch size in ViTs and should take the stride value into consideration in Swins, which has downsampling operations. $q_i, k_{i,+}$ are the feature vectors corresponding to the i_{th} masked patch from the learnable encoder and frozen teacher model, respectively. k_j is the j_{th} feature vector in the *key* queue. K is the length of the *key* queue (4096 by default). τ is a temperature term (0.2 by default). Since patch features are very redundant, for image x , we instead put the average feature of all patch features of the teacher model into the *key* queue.

Image-level Reconstruction Loss. As compensation for the patch-level reconstruction loss, which only focuses on local patch reconstruction, the image-level reconstruction loss here focuses on reconstruction from the global view. We adopt a contrastive loss to encourage the global features between masked and non-masked images to be as similar as possible. The difference from other contrastive learning-based SSL works [9, 43] is that instead of taking two views of a sample as a positive pair, we take the non-masked view x and the masked view (x, m) as a positive pair. For convenience, we denote the projector, predictor, and momentum projector as $\mathbf{p}_1^I, \mathbf{p}_2^I$, and \mathbf{p}_3^I , respectively, which are all 2 layer MLP. The image-level reconstruction loss $\mathcal{L}_{\text{image}}$ is computed as:

$$\mathcal{L}_{\text{image}} = -\log \frac{\exp(q \cdot k_+ / \tau)}{\exp(q \cdot k_+ / \tau) + \sum_{i=1}^K \exp(q \cdot k_i / \tau)}, \quad (3)$$

in which:

$$\begin{cases} q = \mathbf{p}_2^I(\mathbf{p}_1^I(\mathbf{f}(x, m))), \\ k_+ = \mathbf{p}_3^I(\mathbf{f}'(x)), \end{cases} \quad (4)$$

where q, k_+, k_i are all 1-D feature vectors. k_i is the feature of un-masked images in the *key* queue. K is the length of the *key* queue (4096 by default). τ is a temperature term (0.2 by default).

3.3 Implementation

Architecture. We use the Vision Transformers [14] and Swin Transformers [25] as the backbone. For ViTs, we conduct experiments on ViT-S and ViT-B with patch size set to 16. For Swins, we conduct experiments on Swin-T and Swin-B with patch size set to 4 and window size set to 7.

Pre-training Setup. We by default pre-train MimCo on ImageNet-1K training set with AdamW [26] optimizer and a batch size of 2048. For ViT-S and ViT-B, we use the MoCov3 [9] pre-trained models as the contrastive teacher models. For Swin-T and Swin-B, we use the MoBY [43] pre-trained models as the contrastive teacher models. If not specified, we pre-train all architectures with 100 epochs. The learning rate is linearly warmed up during the first 10 epochs to its base value scaled with the total batch size: $\text{lr} = 1e^{-3} \times \text{batch_size} / 512$, and the weight decay is 0.05. A light data augmentation strategy is used: random resize cropping with scale range of [0.67, 1] and an aspect ratio range of [3/4, 4/3], followed

Algorithm 1 Pytorch-like Pseudo-code of MimCo.

Input:

the learnable encoder and frozen contrastive teacher model \mathbf{f}, \mathbf{f}' ;
 # the patch-level projector, momentum projector, and predictor $\mathbf{p}_1^p, \mathbf{p}_3^p, \mathbf{p}_2^p$;
 # the image-level projector, momentum projector, and predictor $\mathbf{p}_1^I, \mathbf{p}_3^I, \mathbf{p}_2^I$;

for x **in** loader **do**

apply weak augmentation on images
 $x = \text{augment}(x)$
 $m = \text{random_mask_generator}(\text{mask_ratio}, \text{patch_size})$
 # extract features for masked and non-masked images
 $z, z_k = \mathbf{f}(x, m), \mathbf{f}'(x)$
 $z_k = z_k.\text{detach}()$

extract features of masked patches: $N \times C$
 $z^p, z_k^p = \mathbf{p}_2^p(\mathbf{p}_1^p(z)), \mathbf{p}_3^p(z_k)$
 $z^p, z_k^p = z^p[m], z_k^p[m]$
 # compute contrastive loss for masked patches
 $\mathcal{L}_{\text{patch}} = \text{contrastive_loss}(z^p, z_k^p, \text{queue_patch})$
 $\text{enqueue_dequeue}(\text{queue_patch}, \text{mean}(z_k^p))$

extract features for whole images: $B \times C$
 $z^I, z_k^I = \text{avg}(z), \text{avg}(z_k)$
 $z^I, z_k^I = \mathbf{p}_2^I(\mathbf{p}_1^I(z^I)), \mathbf{p}_3^I(z_k^I)$
 # compute contrastive loss for images
 $\mathcal{L}_{\text{image}} = \text{contrastive_loss}(z^I, z_k^I, \text{queue_image})$
 $\text{enqueue_dequeue}(\text{queue_image}, z_k^I)$

end for

by a random flipping and a color normalization steps. Following SimMIM [45], the default masking strategy of MimCo is: a random masking strategy with a patch size of 32×32 and a mask ratio of 60%.

4 EXPERIMENTS

We first transfer MimCo to downstream tasks, following the standard evaluation protocols adopted in prior arts. For the classification task on ImageNet-1K, we evaluate the quality of MimCo pre-training with Swin-T, Swin-B, ViT-S and ViT-B as backbones. For other dense tasks, including instance detection and segmentation on MS-COCO, semantic segmentation on ADE20K, we use Swin-T as the backbone to evaluate the transfer performance of MimCo pre-training. We then give a brief ablation study on the crucial composition of MimCo.

4.1 Transferring Performance on Downstream Tasks

Classification on ImageNet-1K. Previous work [19, 45] have shown that the accuracy of linear probing is not always consistent with that of finetuning, especially for MIM-based pretraining methods. In this work, we directly study the finetuning accuracy

Table 1: Finetuning accuracy on ImageNet-1K. *Sup.* denotes the supervised baselines. [†] denotes using multi-crop augmentation. [‡] denotes our pre-training results using official code.

Method	Arch.	Extra model	Pre-train Epochs	Effective Epochs	Top-1 acc (%)
Sup. [25]					81.2
SimMIM [45]	Swin-T		800	800	80.9 [‡]
MoBY [43]			300	600	81.4
MimCo (Ours)		MoBY-Swin-T-300e	100	700	81.7
MimCo (Ours)		MoBY-Swin-T-300e	300	900	81.9
Sup. [25]					
SimMIM [45]	Swin-B		100	100	83.5
SimMIM [45]			800	800	84.0
MoBY [43]			300	600	83.1 [‡]
MimCo (Ours)		MoBY-Swin-B-300e	100	700	84.0
MimCo (Ours)		MoBY-Swin-B-300e	300	900	84.3
Sup. [36]	ViT-S/16				79.9
BEiT [3]		dVAE	800	800	81.4
DINO [5]			800	3200	82.0 [†]
iBOT [47]			800	3200	82.3 [†]
MoCov3 [9]			300	600	81.4
MimCo (Ours)		MoCov3-ViT-S/16-300e	100	700	82.5
MimCo (Ours)		MoCov3-ViT-S/16-300e	300	900	82.7
Sup. [36]		ViT-B/16			
BEiT [3]			800	800	83.2
DINO [5]			400	1600	83.6 [†]
MAE [19]			1600	1600	83.6
SimMIM [45]			800	800	83.8
iBOT [47]			400	1600	83.8 [†]
MoCov3 [9]			300	600	83.2
MimCo (Ours)	MoCov3-ViT-B/16-300e		100	700	83.7
MimCo (Ours)	MoCov3-ViT-B/16-300e		300	900	83.9

on ImageNet-1K dataset. We focus on the comparison with self-supervised methods for Transformers and its supervised baseline. By default, we follow the finetuning protocol in iBOT [47] to use a layer-wise learning rate decay, weight decay and AdamW optimizer. Following the common practice of other self-supervised work, we search the hyperparameters for optimal finetuning performance, as shown in Table 6. Expressly, for Swin-T, we set the layer-wise learning rate decay to 0.75, the drop path rate to 0.1, and the finetuning epoch to 100. For Swin-B, we set the layer-wise learning rate decay to 0.75, the drop path rate to 0.2, and the finetuning epoch to 100. For ViT-S/16, we set the layer-wise learning rate decay to 0.75, the drop path rate to 0.1, and the finetuning epoch to 300. For ViT-B/16, we set the layer-wise learning rate decay to 0.65, the drop path rate to 0.1, and the finetuning epoch to 100.

As shown in Table 1, when pre-trained with 100 epochs, MimCo achieves top-1 accuracies of 81.7%, 84.0%, 82.5%, and 83.7% with Swin-T, Swin-B, ViT-S/16, and ViT-B/16, respectively, outperforming the contrastive teacher models and performing on par with state-of-the-art methods. When pre-trained with 300 epochs, MimCo achieves top-1 accuracies of 81.9%, 84.3%, 82.7%, and 83.9% with Swin-T, Swin-B, ViT-S/16, and ViT-B/16, respectively, reaching new state-of-the-art results.

Due to different training strategies, different methods with the same pre-training epochs actually see different total numbers of

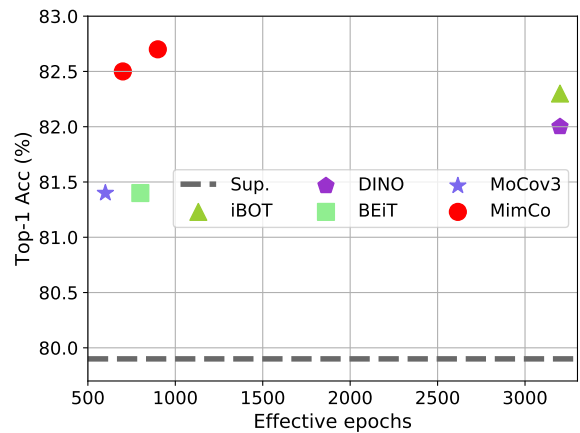


Figure 2: Finetuning accuracy on ImageNet-1K w.r.t. effective pre-training epochs based on ViT-S/16 architecture. Our MimCo exhibits both better transfer performance and higher pre-training efficiency.

images. For fair comparison of pre-training efficiency, we follow iBOT [47] and use *effective pre-training epochs*, defined as actual pre-training epochs multiplied with a scaling factor accounting for

extra trained images. Taking ViT-S as the encoder, as shown in Figure 2, our MimCo achieves a better balance between transfer performance and effective pre-training epochs compared to other pre-training methods.

Object Detection and Instance Segmentation. Mask R-CNN [21] is adopted in the evaluation, following the implementation of [25]. Table 2 shows a comparison of the learned representations of MimCo and other counterparts. MimCo pre-trained with 100 epochs achieves 43.9% AP and 40.1% AP on object detection and instance segmentation, respectively, outperforming sup. and MoBY [43] pre-training. When pre-trained with 300 epochs, the AP for object detection and instance segmentation are further improved to 44.9% and 40.7%, respectively.

Table 2: Results of object detection and instance segmentation finetuned 12 epochs on MS-COCO dataset. We use Mask R-CNN framework with Swin-T as the backbone. * denotes our training result using the official code.

Method	Pre-train Epochs	mAP ^{bbox} (%)	mAP ^{mask} (%)
Sup. [25]	100	41.6*	38.4*
Sup. [25]	300	43.7	39.8
MoBY [43]	100	41.5	38.3
MoBY [43]	300	43.6	39.6
MimCo (Ours)	100	43.9	40.1
MimCo (Ours)	300	44.9	40.7

Semantic Segmentation. The UPerNet [42] segmentation approach and the ADE20K dataset are adopted in the evaluation, following MoBY [43]. Table 3 shows the comparison of MimCo and other pre-training methods on this evaluation. When pre-trained with 300 epochs, MimCo achieve an mIoU of 45.40%, outperforming supervised and other self-supervised pre-training methods.

Table 3: Transfer performance comparison of ADE20K semantic segmentation. All models are finetuned for 160K iterations on the ADE20K dataset, with Swin-T and ViT-B/16 as the backbone and UperNet as the segmentation framework.

Backbone	Method	Pre-train Epochs	mIoU (%)
Swin-T	Sup. [25]		44.51
	SimMIM [45]	800	40.47
	MoBY [43]	300	44.06
	MimCo (Ours)	100	44.44
	MimCo (Ours)	300	45.40
ViT-B/16	Sup. [25]		46.6
	BEiT [3]	800	45.8
	MAE [19]	1600	48.1
	MimCo (Ours)	300	48.91

Nearest Neighbor Retrieval. As shown in Figure 3, we visualize the learned features of pre-trained models using T-SNE tools. We randomly choose 10 classes of ImageNet-1K dataset to visualize for simplicity, the visualization of learned representation shows that our MimCo significantly improves the linear separability of representations compared to SimMIM [45] and MAE [19]. We further evaluate MimCo on the nearest neighbor retrieval task, which is highly correlated with the linear separability of learned representations. We consider the revisited [31] Oxford and Paris image retrieval datasets. They contain 3 different splits of gradual difficulty with query/database pairs. We report the Mean Average Precision (mAP) for the Medium (M) and Hard (H) splits. We compare MimCo with SimMIM [45] following the evaluation protocol as in DINO [5]. As reported in Table 4, MimCo achieves significantly better performance on this task, further validating that the linear separability of the learned representation is improved.

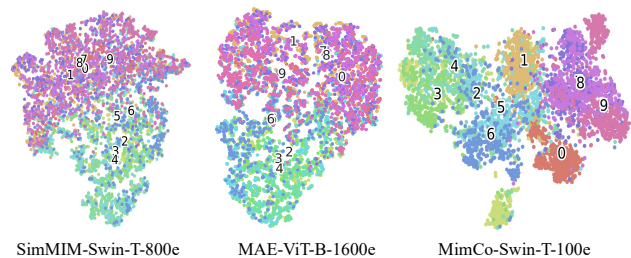


Figure 3: T-SNE feature visualization of MIM method SimMIM [45], MAE [19], and our MimCo on ImageNet-1K dataset. The weights of SimMIM and MAE are from their released pre-trained models.

Table 4: Effect of pre-trained features on nearest neighbor retrieval when using Swin-T as the backbone. The model weights of SimMIM is from our pre-trained model based on the official released code.

Method	Pre-train Epochs	Image Retrieval			
		\mathcal{R}_{Ox}		\mathcal{R}_{Par}	
		M	H	M	H
SimMIM [45]	800	4.23	1.53	8.06	3.13
MimCo (Ours)	100	30.16	7.91	50.82	21.31
MimCo (Ours)	300	28.73	7.81	51.51	22.14

4.2 Ablation Study

Unless otherwise specified, all ablation experiments are pre-trained for 100 epochs on ImageNet-1K dataset with Swin-T as the backbone.

Mask Ratio. For pre-training, we follow the masking strategy in SimMIM [45] by default, which uses a patch size of 32×32 and a mask ratio of 60%. Considering that this masking strategy may not be suitable for our MimCo framework, we study how masking strategy affect the effectiveness of pre-training. We mainly analysis

the effect of mask ratio and report the finetuning accuracy on ImageNet-1K in Table 5. We empirically find that the mask ratio of 60% performs better, and we use it for all other experiments.

Table 5: Effect of mask ratio in our pre-training framework. The patch size is fixed to 32×32 . All experiments are performed with Swin-T as the backbone.

Mask ratio	Top-1 acc (%)
50%	81.56
60%	81.66
70%	81.54

Finetuning Recipes on ImageNet-1K. Following the practice of previous work, we search several critical parameters (mainly the drop path rate and layer-wise learning rate decay) for the best finetuning performance. The ablation results are reported in Table 6.

Table 6: Different finetuning recipes on ImageNet-1K. “L.D.” denotes layer-wise learning rate decay, “D.P.R.” denotes drop path rate.

Arch.	Pre-train Epochs	D.P.R.	L.D.	Top-1 acc (%)
Swin-T	100	0.2	0.75	80.94
		0.1	0.65	81.58
		0.1	0.75	81.66
		0.1	0.85	81.61
Swin-B	100	0.15	0.75	83.79
		0.20	0.75	83.88
		0.25	0.75	83.80
		0.20	0.80	84.04
		0.20	0.85	83.94
ViT-S	100	0.2	0.75	82.28
		0.1	0.65	82.34
		0.1	0.75	82.53
		0.1	0.85	82.49
ViT-B	300	0.2	0.65	83.86
		0.1	0.65	83.89
		0.1	0.7	83.64
		0.1	0.75	83.65

Reconstruction Losses. We first compare our patch-level reconstruction loss with existing work, and then we further experimentally verify the effectiveness of introducing additional image-level reconstruction loss. MaskFeat [40] verifies that reconstructing the features of the pre-trained model with ℓ_1 -loss outperforms reconstructing other targets, including RGB values and HOG features, so we directly compare with the ℓ_1 -loss feature reconstructions. As shown in Table 7, the accuracy of patch reconstruction using contrastive loss reaches 81.55%, outperforming 81.35% of reconstructing patch features with ℓ_1 -loss.

To reveal the importance of additional image-level reconstruction loss $\mathcal{L}_{\text{image}}$ (defined in Equation 3), we conduct factor-by-factor

Table 7: Comparison of losses for reconstructing teacher model features at patch-level. All experiments are pre-trained for 100 epochs and use Swin-T as the backbone.

Patch reconstruction loss	Extra model	Top-1 acc (%)
ℓ_1 loss [40]	MoBY-Swin-T-300e	81.35
Contrastive loss (ours)		81.55

experiments in this section. As shown in Table 8, loss $\mathcal{L}_{\text{patch}}$ and loss $\mathcal{L}_{\text{image}}$ achieve 81.55% and 81.59% top-1 accuracies, respectively, outperforming the supervised pre-training of 81.2% and the MoBY teacher model of 81.40%. When using both losses, MimCo achieves the best results of 81.66% top-1 accuracy.

Table 8: Ablation experiments on the patch- and image-level reconstruction loss terms of MimCo. Image classification results finetuned on ImageNet-1K are reported. All experiments are pre-trained for 100 epochs and use Swin-T as the backbone.

Reconstruction losses		ImageNet-1K Top-1 (%)
$\mathcal{L}_{\text{patch}}$	$\mathcal{L}_{\text{image}}$	
✓		81.55
	✓	81.59
✓	✓	81.66

Table 9: Ablation experiments on the patch- and image-level reconstruction loss terms of MimCo. The results on the revisited Oxford and Paris image retrieval datasets are reported. All experiments are pre-trained for 100 epochs and use Swin-T as the backbone.

Reconstruction losses		Image Retrieval			
$\mathcal{L}_{\text{patch}}$	$\mathcal{L}_{\text{image}}$	\mathcal{ROx}		\mathcal{RPar}	
		M	H	M	H
✓		22.46	5.5	39.16	14.55
	✓	31.58	9.04	53.26	24.07
✓	✓	30.16	7.91	50.82	21.31

Comparison with Multi-task Learning. A simple solution to combine contrastive learning and MIM is through multi-task learning. We use “SimMIM + MoBY” to represent combining two pre-training methods of SimMIM [45] and MoBY [43] through multi-task learning. As shown in Table 10, our MimCo achieves higher performance than the naive multi-task learning method under the same effective pre-training epoch.

Remove Mask Operation. To investigate whether MIM plays an important role in our pre-training framework, we try to remove

Table 10: Comparison with multi-tasking learning approach. All models take Swin-T as the backbone and are finetuned for 100 epochs on the ImageNet-1K dataset.

Method	Extra model	Pre-train Epochs	Effective Epochs	Top-1 acc (%)
SimMIM + MoBY	-	100	300	81.06
SimMIM + MoBY	-	300	900	81.29
MimCo (Ours)	MoBY-Swin-T-300e	100	700	81.66
MimCo (Ours)	MoBY-Swin-T-300e	300	900	81.86

Table 11: Effect of masking input in our pre-training framework. All experiments are performed with Swin-T as the backbone.

Masking image input	Top-1 acc (%)
	81.23
✓	81.66

the masking operation. In fact, our pre-training framework degenerates to a knowledge distillation framework when the masking operation is removed. As shown in Table 11, without masking input, the performance degenerates from 81.66% to 81.23%, indicating the critical role of masking operation in our framework.

5 DISCUSSION

What Semantic Patterns Does MimCo Learn? To further help reveal what patterns does MIM learn, we follow the visualization of iBOT [47] to explore the learned patterns of the pre-trained models of SimMIM [45], MAE [19], and our MimCo via visualization, respectively. Specifically, we use the pre-trained ViT-S/16 models and visualize the top-36 most similar patches (among different images) with the highest cosine similarity on ImageNet-1K validation set. To better understand each little patch, we visualize a 80×80 context for each 16×16 patch (highlight in orange color). As depicted in Figure 4, the top left patch in each pattern layout is used as the query patch. For all patterns, the MIM methods SimMIM [45] and MAE [19] tend to group the patches with similar colors regardless of their semantic meaning. This might be because they use the raw pixels as the learning target of the masked patches, which force the model to focus on learning the low-level details (e.g., color) and ignore high-level semantics. It is worth noting that, our MimCo is capable of excavating more clear and meaningful semantic patterns, e.g., head of person, head of birds, and colorful flowers. In addition to specific objects, the first row shows that MimCo can successfully group text on different backgrounds. The results indicate that MimCo can learn both low-level details and high-level semantics at the same time.

6 CONCLUSIONS

This work proposes a novel MIM pre-training framework, named MimCo, which leverages contrastive teacher models to improve the linear separability of learned representations, thereby improving pre-training performance. MimCo is flexible and efficient: 1)

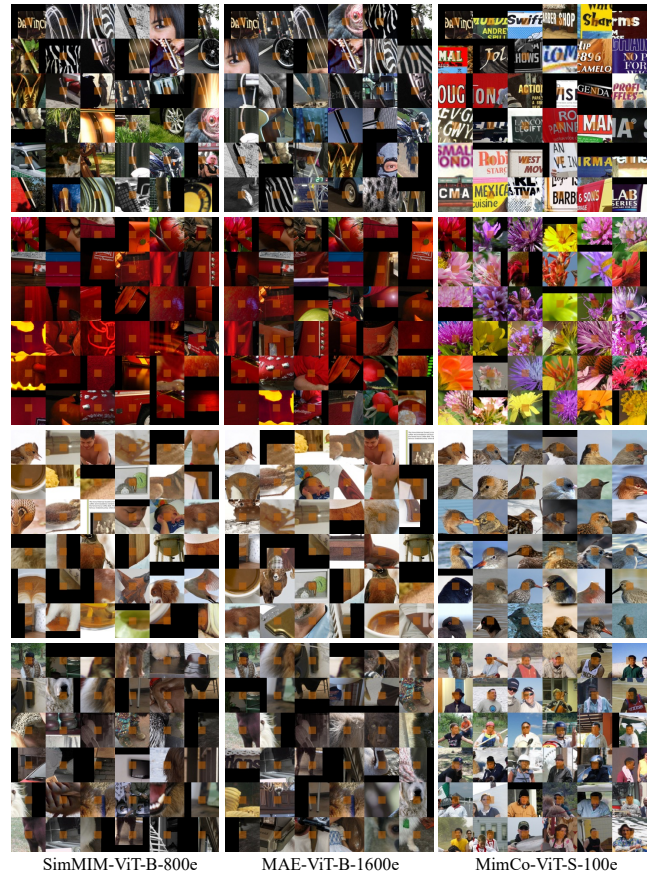


Figure 4: Visualization of semantic patterns. The top left patch is used as the query patch in each pattern layout. “SimMIM-ViT-B-800e” and “MAE-ViT-B-1600e” are from their official released pre-trained models with 800 and 1600 epochs, respectively.

the contrastive teacher model can be flexibly substituted; 2) simple weak data augmentation is used for pre-training; 3) MimCo achieves state-of-the-art transfer performance with fewer effective pre-training epochs. We hope that our strong results and flexible pre-training framework will facilitate pre-training research, especially combining different pre-training pretext tasks such as contrastive learning and MIM.

REFERENCES

- [1] Dosovitskiy Alexey, Philipp Fischer, Jost Tobias, Martin Riedmiller Springenberg, and Thomas Brox. 2016. Discriminative, unsupervised feature learning with exemplar convolutional, neural networks. *IEEE TPAMI* 38, 9 (2016), 1734–1747.
- [2] Jimmy Ba and Rich Caruana. 2014. Do deep nets really need to be deep? *Advances in neural information processing systems (NIPS)* 27 (2014).
- [3] Hangbo Bao, Li Dong, and Furu Wei. 2021. Beit: Bert pre-training of image transformers. *arXiv preprint arXiv:2106.08254* (2021).
- [4] Yue Cao, Zhenda Xie, Bin Liu, Yutong Lin, Zheng Zhang, and Han Hu. 2020. Parametric instance classification for unsupervised visual feature learning. *Advances in neural information processing systems (NeurIPS)* 33 (2020), 15614–15624.
- [5] Mathilde Caron, Hugo Touvron, Ishan Misra, Hervé Jégou, Julien Mairal, Piotr Bojanowski, and Armand Joulin. 2021. Emerging properties in self-supervised vision transformers. In *Proceedings of the IEEE/CVF International Conference on Computer Vision (ICCV)*. 9650–9660.
- [6] Mark Chen, Alec Radford, Rewon Child, Jeffrey Wu, Heewoo Jun, David Luan, and Ilya Sutskever. 2020. Generative pretraining from pixels. In *International Conference on Machine Learning (ICML)*. 1691–1703.
- [7] Ting Chen, Simon Kornblith, Mohammad Norouzi, and Geoffrey Hinton. 2020. A simple framework for contrastive learning of visual representations. In *International conference on machine learning*. PMLR, 1597–1607.
- [8] Ting Chen, Simon Kornblith, Kevin Swersky, Mohammad Norouzi, and Geoffrey E Hinton. 2020. Big self-supervised models are strong semi-supervised learners. *Advances in neural information processing systems* 33 (2020), 22243–22255.
- [9] Xinlei Chen, Saining Xie, and Kaiming He. 2021. An empirical study of training self-supervised vision transformers. In *Proceedings of the IEEE/CVF International Conference on Computer Vision (ICCV)*. 9640–9649.
- [10] Navneet Dalal and Bill Triggs. 2005. Histograms of oriented gradients for human detection. In *2005 IEEE computer society conference on computer vision and pattern recognition (CVPR'05)*, Vol. 1. Ieee, 886–893.
- [11] Jacob Devlin, Ming-Wei Chang, Kenton Lee, and Kristina Toutanova. 2018. Bert: Pre-training of deep bidirectional transformers for language understanding. *arXiv preprint arXiv:1810.04805* (2018).
- [12] Carl Doersch, Abhinav Gupta, and Alexei A Efros. 2015. Unsupervised visual representation learning by context prediction. In *Proceedings of the IEEE international conference on computer vision (ICCV)*. 1422–1430.
- [13] Xiaoyi Dong, Jianmin Bao, Ting Zhang, Dongdong Chen, Weiming Zhang, Lu Yuan, Dong Chen, Fang Wen, and Nenghai Yu. 2021. PeCo: Perceptual Codebook for BERT Pre-training of Vision Transformers. *arXiv preprint arXiv:2111.12710* (2021).
- [14] Alexey Dosovitskiy, Lucas Beyer, Alexander Kolesnikov, Dirk Weissenborn, Xi-aohua Zhai, Thomas Unterthiner, Mostafa Dehghani, Matthias Minderer, Georg Heigold, Sylvain Gelly, et al. 2020. An image is worth 16x16 words: Transformers for image recognition at scale. *arXiv preprint arXiv:2010.11929* (2020).
- [15] Alexey Dosovitskiy, Jost Tobias Springenberg, Martin Riedmiller, and Thomas Brox. 2014. Discriminative unsupervised feature learning with convolutional neural networks. *Advances in neural information processing systems (NIPS)* 27 (2014).
- [16] Zhiyuan Fang, Jianfeng Wang, Lijuan Wang, Lei Zhang, Yezhou Yang, and Zicheng Liu. 2021. SEED: Self-supervised Distillation For Visual Representation. In *ICLR*.
- [17] Spyros Gidaris, Praveer Singh, and Nikos Komodakis. 2018. Unsupervised representation learning by predicting image rotations. *arXiv preprint arXiv:1803.07728* (2018).
- [18] Jean-Bastien Grill, Florian Strub, Florent Altché, Corentin Tallec, Pierre Richemond, Elena Buchatskaya, Carl Doersch, Bernardo Avila Pires, Zhaohan Guo, Mohammad Gheshlaghi Azar, et al. 2020. Bootstrap your own latent—a new approach to self-supervised learning. *Advances in Neural Information Processing Systems (NeurIPS)* 33 (2020), 21271–21284.
- [19] Kaiming He, Xinlei Chen, Saining Xie, Yanghao Li, Piotr Dollár, and Ross Girshick. 2021. Masked autoencoders are scalable vision learners. *arXiv preprint arXiv:2111.06377* (2021).
- [20] Kaiming He, Haoqi Fan, Yuxin Wu, Saining Xie, and Ross Girshick. 2020. Momentum contrast for unsupervised visual representation learning. In *Proceedings of the IEEE/CVF conference on computer vision and pattern recognition (CVPR)*. 9729–9738.
- [21] Kaiming He, Georgia Gkioxari, Piotr Dollár, and Ross Girshick. 2017. Mask r-cnn. In *Proceedings of the IEEE international conference on computer vision (ICCV)*. 2961–2969.
- [22] Kaiming He, Xiangyu Zhang, Shaoqing Ren, and Jian Sun. 2016. Deep residual learning for image recognition. In *CVPR*. 770–778.
- [23] Geoffrey Hinton, Oriol Vinyals, Jeff Dean, et al. 2015. Distilling the knowledge in a neural network. *arXiv preprint arXiv:1503.02531* 2, 7 (2015).
- [24] Soroush Abbasi Koohpayegani, Ajinkya Tejankar, and Hamed Pirsiavash. 2020. CompRes: Self-Supervised Learning by Compressing Representations. In *NeurIPS*, Hugo Larochelle, Marc'Aurelio Ranzato, Raia Hadsell, Maria-Florina Balcan, and Hsuan-Tien Lin (Eds.).
- [25] Ze Liu, Yutong Lin, Yue Cao, Han Hu, Yixuan Wei, Zheng Zhang, Stephen Lin, and Baining Guo. 2021. Swin Transformer: Hierarchical Vision Transformer using Shifted Windows. In *ICCV*. IEEE, 9992–10002. <https://doi.org/10.1109/ICCV48922.2021.00986>
- [26] Ilya Loshchilov and Frank Hutter. 2019. Decoupled Weight Decay Regularization. In *7th International Conference on Learning Representations, ICLR 2019, New Orleans, LA, USA, May 6-9, 2019*. OpenReview.net. <https://openreview.net/forum?id=Bkg6RiCqY7>
- [27] Mehdi Noroozi and Paolo Favaro. 2016. Unsupervised learning of visual representations by solving jigsaw puzzles. In *European conference on computer vision (ECCV)*. Springer, 69–84.
- [28] Mehdi Noroozi, Ananth Vinjimoor, Paolo Favaro, and Hamed Pirsiavash. 2018. Boosting self-supervised learning via knowledge transfer. In *Proceedings of the IEEE Conference on Computer Vision and Pattern Recognition (CVPR)*. 9359–9367.
- [29] Deepak Pathak, Ross Girshick, Piotr Dollár, Trevor Darrell, and Bharath Hariharan. 2017. Learning features by watching objects move. In *Proceedings of the IEEE conference on computer vision and pattern recognition (CVPR)*. 2701–2710.
- [30] Deepak Pathak, Philipp Krahenbuhl, Jeff Donahue, Trevor Darrell, and Alexei A Efros. 2016. Context encoders: Feature learning by inpainting. In *Proceedings of the IEEE conference on computer vision and pattern recognition*. 2536–2544.
- [31] Filip Radenovic, Ahmet Iscen, Giorgos Tolias, Yannis Avrithis, and Ondrej Chum. 2018. Revisiting Oxford and Paris: Large-Scale Image Retrieval Benchmarking. In *2018 IEEE Conference on Computer Vision and Pattern Recognition, CVPR 2018, Salt Lake City, UT, USA, June 18-22, 2018*. Computer Vision Foundation / IEEE Computer Society, 5706–5715.
- [32] Alec Radford, Karthik Narasimhan, Tim Salimans, and Ilya Sutskever. 2018. Improving language understanding by generative pre-training. (2018).
- [33] Aditya Ramesh, Mikhail Pavlov, Gabriel Goh, Scott Gray, Chelsea Voss, Alec Radford, Mark Chen, and Ilya Sutskever. 2021. Zero-shot text-to-image generation. In *International Conference on Machine Learning (ICML)*. PMLR, 8821–8831.
- [34] Adriana Romero, Nicolas Ballas, Samira Ebrahimi Kahou, Antoine Chassang, Carlo Gatta, and Yoshua Bengio. 2014. Fitnets: Hints for thin deep nets. *arXiv preprint arXiv:1412.6550* (2014).
- [35] Yonglong Tian, Dilip Krishnan, and Phillip Isola. 2019. Contrastive representation distillation. *arXiv preprint arXiv:1910.10699* (2019).
- [36] Hugo Touvron, Matthieu Cord, Matthijs Douze, Francisco Massa, Alexandre Sablayrolles, and Herve Jegou. 2021. Training data-efficient image transformers and distillation through attention. In *Proceedings of the 38th International Conference on Machine Learning (ICML) (Proceedings of Machine Learning Research, Vol. 139)*, Marina Meila and Tong Zhang (Eds.). PMLR, 10347–10357.
- [37] Aaron Van den Oord, Yazhe Li, and Oriol Vinyals. 2018. Representation learning with contrastive predictive coding. *arXiv e-prints* (2018), arXiv:1807.
- [38] Ashish Vaswani, Noam Shazeer, Niki Parmar, Jakob Uszkoreit, Llion Jones, Aidan N Gomez, Lukasz Kaiser, and Illia Polosukhin. 2017. Attention is all you need. *Advances in neural information processing systems (NIPS)* 30 (2017).
- [39] Xiaolong Wang and Abhinav Gupta. 2015. Unsupervised learning of visual representations using videos. In *Proceedings of the IEEE international conference on computer vision (ICCV)*. 2794–2802.
- [40] Chen Wei, Haoqi Fan, Saining Xie, Chao-Yuan Wu, Alan Yuille, and Christoph Feichtenhofer. 2021. Masked Feature Prediction for Self-Supervised Visual Pre-Training. *arXiv:2112.09133 [cs.CV]*
- [41] Zhirong Wu, Yuanjun Xiong, Stella X Yu, and Dahua Lin. 2018. Unsupervised feature learning via non-parametric instance discrimination. In *Proceedings of the IEEE conference on computer vision and pattern recognition (CVPR)*. 3733–3742.
- [42] Tete Xiao, Yingcheng Liu, Bolei Zhou, Yuning Jiang, and Jian Sun. 2018. Unified perceptual parsing for scene understanding. In *Proceedings of the European Conference on Computer Vision (ECCV)*. 418–434.
- [43] Zhenda Xie, Yutong Lin, Zhuliang Yao, Zheng Zhang, Qi Dai, Yue Cao, and Han Hu. 2021. Self-Supervised Learning with Swin Transformers. *arXiv:2105.04553 [cs.CV]*
- [44] Zhenda Xie, Yutong Lin, Zheng Zhang, Yue Cao, Stephen Lin, and Han Hu. 2021. Propagate yourself: Exploring pixel-level consistency for unsupervised visual representation learning. In *Proceedings of the IEEE/CVF Conference on Computer Vision and Pattern Recognition (CVPR)*. 16684–16693.
- [45] Zhenda Xie, Zheng Zhang, Yue Cao, Yutong Lin, Jianmin Bao, Zhuliang Yao, Qi Dai, and Han Hu. 2021. SimMIM: A Simple Framework for Masked Image Modeling. *arXiv:2111.09886 [cs.CV]*
- [46] Richard Zhang, Phillip Isola, and Alexei A Efros. 2016. Colorful image colorization. In *European conference on computer vision (ECCV)*. Springer, 649–666.
- [47] Jinghao Zhou, Chen Wei, Huiyu Wang, Wei Shen, Cihang Xie, Alan Yuille, and Tao Kong. 2021. ibot: Image bert pre-training with online tokenizer. *arXiv preprint arXiv:2111.07832* (2021).